Thin Solid Films 557 (2014) 342–345

Contents lists available at ScienceDirect

Thin Solid Films

journal homepage: www.elsevier.com/locate/tsf

Fabrication and evaluation of propagation loss of Si/SiGe/Si photonic-wire waveguides for Si based optical modulator

Younghyun Kim [a,*], Mitsuru Takenaka [a], Takenori Osada [b], Masahiko Hata [b], Shinichi Takagi [a]

[a] Department of Electrical Engineering and Information Systems, The University of Tokyo, 7-3-1 Hongo, Bunkyo-ku, Tokyo 113-8656, Japan
[b] Sumitomo Chemical Co. Ltd., 6 Kitahara, Tsukuba, Ibaraki 300-3294, Japan

ARTICLE INFO

Available online 25 October 2013

Keywords:
Si/SiGe/Si optical modulator
Si/SiGe/Si heterostructure
Si/SiGe/Si photonic-wire waveguide
Si/SiGe/Si waveguide core
Strained SiGe
Bandgap narrowing
Si-based optical modulator
Optoelectronic integrated circuits

ABSTRACT

We have characterized photonic-wire waveguides with Si/SiGe/Si heterostructure ribs for Si-based optical modulators. The Si (80 nm)/$Si_{0.72}Ge_{0.28}$ (40 nm) layers grown on Si-on-insulator by molecular beam epitaxy for optical modulators were evaluated by *in-situ* reflection high-energy electron diffraction, atomic force microscope, X-ray diffraction and Raman spectroscopy, exhibiting that the fully-strained highly-crystalline SiGe layer was obtained. We have evaluated the propagation loss of the Si/strained SiGe/Si photonic-wire waveguides. The wavelength dependence of the propagation loss exhibits the bandgap narrowing of the strained $Si_{0.72}Ge_{0.28}$, while the optical absorption of the strained $Si_{0.72}Ge_{0.28}$ is not significant for the optical modulator application at 1.55-μm wavelength.

1. Introduction

Recently, silicon (Si) optical modulators have attracted much attention as one of the fundamental building blocks for optoelectronic integrated circuits toward large-scaled integrated circuits with on-chip optical interconnects [1–3]. High speed optical modulators have recently been demonstrated so far by using a Mach–Zehnder interferometer (MZI) with phase-shifters in which the effective refractive index of the Si waveguide is modulated by the electrical signal. An MZI has been mostly used for getting optical modulation because of its wide wavelength bandwidth, while the large device length of several millimeters is considered as one of the most challenging problems for large scale integration [4–6].

To solve this problem, strained SiGe-based optical modulators have been proposed [7,8]. The refractive index change from the plasma dispersion effect is inversely proportional to conductivity effective masses of electrons and holes [9]. Therefore, the lighter conductivity masses become, the larger plasma dispersion occurs. Compressively strained SiGe, which is one of the promising materials for future scaled p-channel metal-oxide-semiconductor (MOS) transistors [10–12], is well known to exhibit the light conductivity hole mass. Thus, the plasma dispersion effect is expected to be enhanced through effective mass modulation in strained SiGe, enabling small device footprint. In our previous work [8], the strain effect on carrier-injection type optical modulators by using the Si/strained SiGe/Si waveguide is numerically investigated. Owing to enhancement in free-carrier effects, the plasma dispersion effect and free-carrier absorption, of strained SiGe, the pin-junction $Si/SiGe_{0.28}/Si$ optical modulator has approximately 4.5× smaller switching power than that of the Si modulator. However, the bandgap energy decreases with an increase in the Ge fraction of SiGe, causing an increase in optical absorption at 1.55-μm wavelength [13,14]. In this paper, we have fabricated Si/strained $Si_{0.72}Ge_{0.28}$/Si heterostructures on a silicon-on-insulator (SOI) wafer by molecular beam epitaxy (MBE), and evaluated the propagation loss of the Si/SiGe/Si photonic-wire waveguides for optical modulator applications at 1.55-μm wavelength.

2. Experiment

2.1. Device fabrication

We show the process flow of the Si/SiGe/Si photonic-wire waveguide in Fig. 1. The Si/SiGe/Si–OI substrate was prepared by using a (001) SOI wafer with a 2-μm-thick buried oxide layer (BOX). First, a 220-nm-thick SOI layer was thinned to be 100 nm by thermal oxidation at 1100 °C and BHF etching of a thermally grown SiO_2 layer as shown in Fig. 1(a) and (b). Then, a 40-nm-thick $Si_{0.72}Ge_{0.28}$ layer and an 80-nm-thick Si layer were grown on the SOI by MBE under the base pressure of 3×10^{-8} Pa at 400 °C and 600 °C, respectively as shown in Fig. 1(c). The thickness of the SiGe layer was kept below the critical thickness for avoiding strain relaxation [15]. Then, photonic-wire waveguides with a Si/SiGe mesa were fabricated by using the Si/SiGe/Si–OI wafer. After cleaning the substrate, the electron beam resist (ZEP520A) was coated on the substrate with the spin condition of 3000 rpm for 30 s followed by the prebake at 160 °C for 10 min and deep ultraviolet (DUV) lithography. Then, waveguide patterns of variable waveguide widths were formed by reactive ion etching

* Corresponding author.
E-mail address: yhkim@mosfet.t.u-tokyo.ac.jp (Y. Kim).

0040-6090/$ – see front matter
http://dx.doi.org/10.1016/j.tsf.2013.10.063

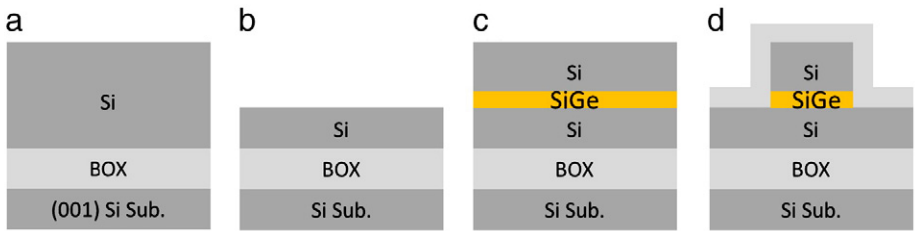

Fig. 1. Process flow of Si/SiGe/Si photonic-wire waveguide. (a) initial 220-nm-thick SOI, (b) 100-nm-thick SOI thinned by thermal oxidation, (c) Si/SiGe/Si–OI grown by MBE, and (d) dry etching of waveguide mesa, followed by SiO_2 passivation.

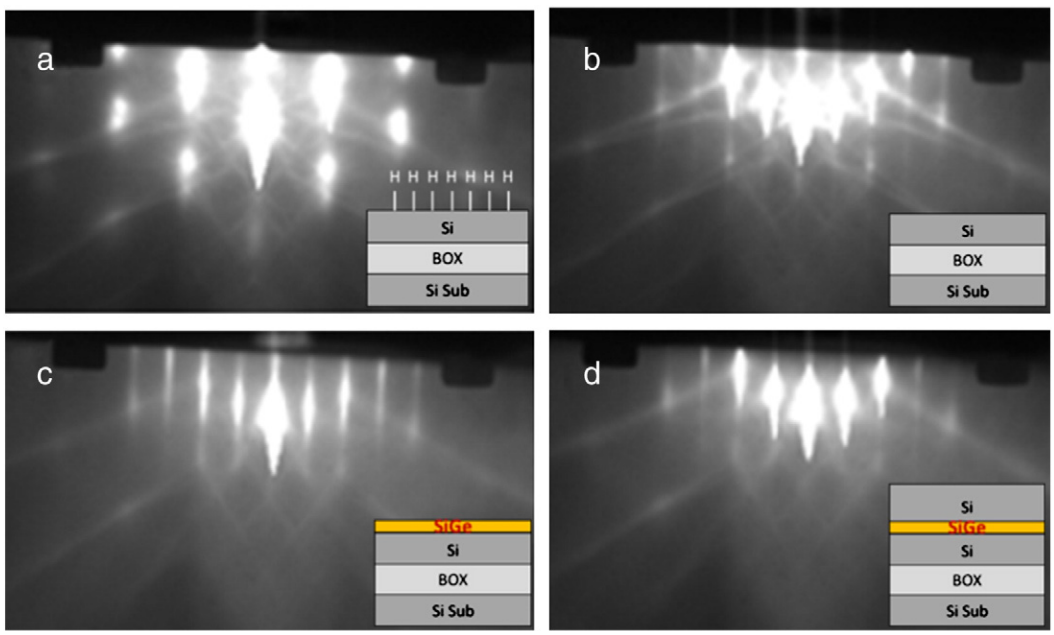

Fig. 2. *in-situ* RHEED images during MBE growth procedures: after (a) SOI installation, (b) thermal cleaning, (c) SiGe growth, and (d) Si growth.

with CF_4 gas for approximately 11 min. The gas pressure of CF_4 and RF power were set to be 1 Pa and 20 W, respectively. Finally, a 500-nm-thick SiO_2 layer was deposited by plasma-enhanced chemical vapor deposition for device passivation as shown in Fig. 1(d). Si photonic-wire waveguides as a control sample were also fabricated by using the 220-nm-thick SOI substrate, which is corresponding to the total thickness of the 80-nm-thick Si/40-nm-thick SiGe/100-nm-thick Si waveguide.

2.2. Characterization of epitaxially grown Si/SiGe/Si–OI and device

Fig. 2 shows the *in-situ* reflection high-energy electron diffraction (RHEED) images during the crystal growth process of Si/SiGe on the SOI substrate. The as-installed sample shows the spotty 1 × 1 RHEED pattern due to hydrogen termination during BHF as shown in Fig. 2(a). Fig. 2(b) shows the longish 2 × 1 RHEED pattern after thermal cleaning at 850 °C for 30 min, meaning that hydrogen was removed by high thermal energy. Fig. 2(c) and (d) show the longish 2 × 1 RHEED patterns during the SiGe and Si growth, indicating the two dimensional island morphology.

Fig. 3 shows the surface morphologies of the Si/SiGe/SOI substrate measured by atomic force microscope (AFM, Nanocute SS, Dynamic force mode). The root-mean-squares of the surface roughness with the scanning areas of (a) 500 × 500 nm^2, (b) 5 × 5 μm^2, and (c) 10 × 10 μm^2 are less than 0.18 nm, indicating that the pseudomorphic strained SiGe layer is obtained.

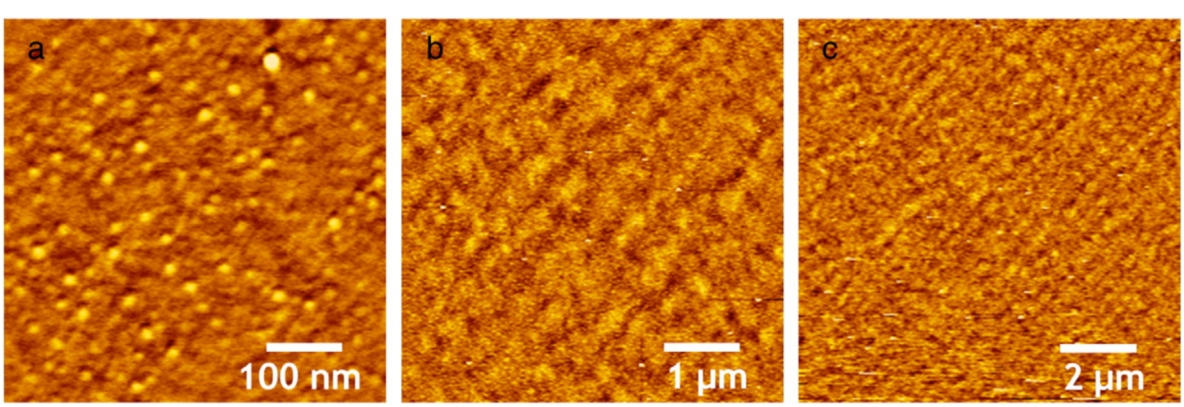

Fig. 3. AFM evaluation of surface roughnesses of the Si/SiGe/SOI samples grown by MBE with the scanning areas of (a) 500 × 500 nm^2, (b) 5 × 5 μm^2, and (c) 10 × 10 μm^2.